Effect of nanocellulose on the structure and properties of arrowroot starch films

Abdul Halim Muhammad Firdaus[1] (ORCID ID: 0009-0004-4853-1449), **Salit Mohd Sapuan**[1] (0000-0002-4598-6358), **Edi Syams Zainudin**[1,*] (0000-0001-7425-4183), **Mohd Afdzaluddin Atiqah**[2] (0000-0003-0583-7486), **Muhammad Hafiz Imran Bin Mohammad Fadzil**[1], **Vasi Uddin Siddiqui**[1] (0000-0003-3427-8943)

DOI: https://doi.org/10.14314/polimery.2026.2.5

Abstract: Effect of 1 and 3 wt% nanocrystalline arrowroot cellulose (ARNC) on the structure and properties of arrowroot starch (AS)-based films was investigated. The addition of ARNC increased the film density and reduced its water absorption, indicating improved moisture barrier properties. Furthermore, tensile strength increased (from 2.5 MPa to 4.3 MPa) and elongation at break (from 13.4% to 45%). Simultaneously, Young's modulus decreased (from 65.7 MPa to 32.5 MPa), suggesting increased flexibility. FESEM analysis revealed good dispersion of cellulose nanocrystals in the composite, with a tendency to agglomerate at higher ARNC content.

Keywords: nanocrystalline cellulose, nanocellulose, biopolymer, arrowroot.

Wpływ nanocelulozy na strukturę i właściwości folii na bazie skrobi z maranty trzcinowej

Streszczenie: Zbadano wpływ dodatku 1 i 3% mas. nanokrystalicznej celulozy z maranty trzcinowej (ARNC) na strukturę i właściwości folii na bazie skrobi z maranty trzcinowej (AS). Dodatek ARNC zwiększył gęstość folii i zmniejszył jej absorpcję wody, co wskazuje na poprawę właściwości barierowych dla wilgoci. Ponadto, wzrosła wytrzymałość na rozciąganie (z 2,5 MPa do 4,3 MPa) oraz wydłużenie przy zerwaniu (z 13,4% do 45%). Jednocześnie nastąpiło zmniejszenie modułu Younga (z 65,7 MPa do 32,5 MPa), co sugeruje większą elastyczność. Analiza FESEM wykazała dobrą dyspersję nanokryształów celulozy w kompozycie z tendencją do aglomeracji przy większej zawartości ARNC.

Słowa kluczowe: nanokrystaliczna celuloza, nanoceluloza, biopolimer, maranta trzcinowa.

The growing environmental awareness of the world has made the call to purchase sustainable products and environmentally friendly products even stronger. An exciting approach to fulfill this need is by designing bio-based materials, which cover a wide range of substances including biopolymers, natural fibers and biocomposites. Manu *et al.* describe a biocomposite as an amalgamation of a natural, in many cases, biological reinforcement substance with a polymer matrix that can be either natural or synthetic [1]. Essentially, a biopolymer composite consists of a biodegradable polymer backbone, which is based on renewable sources, and reinforced with performance enhancing agents that must remain environmentally sustainable [2]. Udayakumar *et al.* also emphasized the importance of the fact that biopolymer composites are generally created by embedding natural fibers as fillers into biodegradable polymer matrices [3]. Biomaterials based on natural resources have recently enjoyed a significant amount of research focus due to their availability and cost-efficiency.

Nanocellulose fibers are one of the most outstanding due to their unique characteristics and the broad scope of applications. It is these nanoscale cellulose fibrils or crystals that confer high strength, stiffness, and biodegradability to bio-based materials making them highly appealing to a wide variety of industries. Their small sizes, at nanoscale, aid the creation of smooth composites with improved physicochemical and mechanical properties [4]. To be precise, addition of nanocellulose made of arrowroot fibers has been demonstrated to enhance flexibility, thus extending the range of applications of these materials in different industrial markets [5]. Tarique *et al.* reported that arrowroot fibers have small diameters, which make them have a high tear resistance and thus useful in packaging and production of tissue papers [6].

[1] Department of Mechanical and Manufacturing Engineering, Faculty of Engineering, Universiti Putra Malaysia (UPM), Serdang 43400, Selangor, Malaysia.

[2] (IMEN) Institute of Microengineering and Nanoelectronics, Universiti Kebangsaan Malaysia (UKM), Bangi 43600, Selangor, Malaysia.

[*] Author for correspondence: edisyam@upm.edu.my

Arrowroot (*Maranta arundinacea*) is a tropical plant, which has this reason; it contains a high percentage of starch, but more importantly its residue fiber is rich in a significant percentage of cellulose and thus it is a potential source of nanocellulose extraction but less exploited [7]. Arrowroot Nanocrystalline Cellulose (ARNC) has a high crystallinity level, high mechanical strength, and good thermal stability and is produced by controlled acid hydrolysis, making it comparable with other traditional sources of cellulose, including wood or bamboo [8]. ARNC is therefore a viable solution towards biodegradable and high-performance biopolymer composite development [9]. Despite the wide theoretical research on starch-based nanocomposites, the use of ARNC in arrowroot starch (AS) to produce a single-origin biopolymer film has not been achieved so far. This new combination is expected to increase the mechanical, thermal, and piezoelectric properties of the film, through enhanced interfacial compatibility, and crystalline alignment, thereby providing a new and arrowroot-derived system of materials that could be used in environmentally sustainable packaging and flexible electronics.

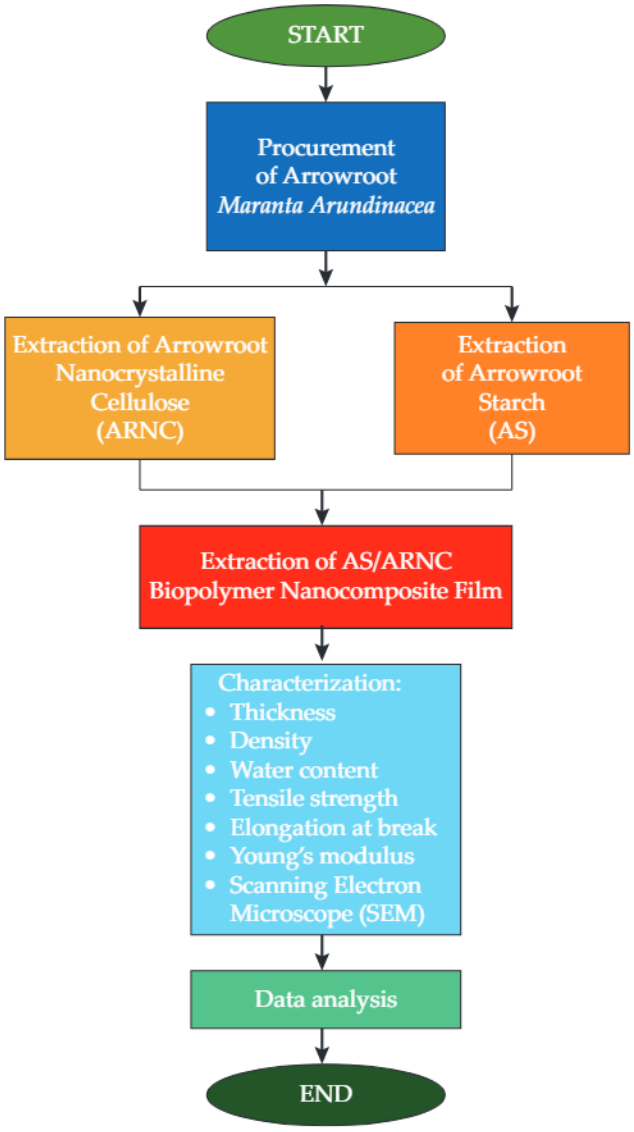

Fig. 1. Project flowchart

Arrowroot starch (AS) is a biopolymer that can be used to create lightweight composite because it has special characteristics and is versatile, as it is produced by using the rhizomes of the plant, Maranta arundinacea [10]. Arrowroot is a high starch source that produces a readily digested starch with high gelling potential and a high amylose content (35.20 %) [11]. These properties make it very appropriate in forming the films, which have improved mechanical and barricade properties than amylopectin [12]. Its high gelling strength is used to advantage in food-based applications to improve texture and stability, and its high amylose content is used to support the development of environmentally friendly packaging films [13]. In that respect, the present research aims at exploring the impact of arrowroot nanocrystalline cellulose (ARNC) reinforcement of AS based biopolymers on the creation of a film.

Even though several studies have been conducted to investigate the incorporation of arrowroot cellulose fibers alongside AS to obtain biopolymer composite materials as substitutes to traditional polymers, there are few studies that focus on incorporating nanocellulose arrowroot fibers into the biopolymer composite materials [14]. Although it could potentially enhance the performance of materials to a substantial degree, the contribution made by nanocellulose reinforcement to AS-based composites has not been thoroughly studied.

This knowledge gap limits our understanding of the potential of using arrowroot nanocellulose fibers to improve the mechanical, physical, and functional properties of starch composites. Therefore, further research is necessary to fully realize their potential and develop sustainable biopolymer materials that could replace traditional plastics.

The aim of this study was to investigate the effect of ARNC on the structure and properties of AS-based films. The process involves AS extraction and extraction of crystalline arrowroot nanocellulose by acid hydrolysis, preparing composites with varying nanocellulose filler content, from 0 to 3 wt%, using the solution casting method to obtain films with a 30 wt% of plasticizers (glycerol and sorbitol). Tensile properties of these nanocomposites were assessed and their morphology analyzed using a field emission scanning electron microscope (FESEM). Additionally, physical properties such as density, thickness, and water content were examined. Figure 1 shows the process flow diagram for this project.

EXPERIMENTAL PART

Materials

The material used for this project is arrowroot (Maranta arundinacea), purchased from a local market at Kuala Lumpur Wholesale Market that imported the arrowroot from Thailand. Glycerol and sorbitol provided by R&M

Fig. 2. Image of arrowroot

Chemical and is distributed by Evergeen Engineering and Resources in Malaysia. Plasticizers were used to influence the hydrophilicity, water vapor permeability and mechanical strength of the film [15]. Moreover, glycerol was added to reduce brittle nature and fragility of non-plasticized AS films [14]. In addition, the application of glycerol as a plasticizer could decrease intermolecular forces and increase the mobility of biopolymers, consequently improving the creation of a more pliable and flexible edible film [16]. A 1:1 mix of 30 wt% blended glycerol and sorbitol (w/w, starch basis) was used. The arrowroot is depicted in Figure 2.

Sample preparation

Arrowroot starch extraction

The first stage involved the selection of fresh arrowroots, peeling, and cutting them into small parts. The resulting pieces were then blended with a Toshiba countertop blender with the presence of distilled water in a 1:2 (m/m) ratio of rhizome to water for 5 min to obtain a uniform slurry. This slurry was filtered through a double-layered cotton cloth to separate the fibrous residue from the starch-rich extract [17]. To ensure maximum starch recovery, the residue was rinsed three times with distilled water, facilitating fiber removal. The filtrate was left undisturbed for approximately 12 hours to allow the starch to settle [18]. Once sedimentation was complete, the excess water was decanted, and the collected starch was dried in an air-flow oven at 60°C for four hours. Figure 3 shows the process of AS extraction.

Arrowroot nanocrystalline cellulose extraction

As highlighted by Tarique *et al.*, arrowroot tubers are composed of two fiber types, namely arrowroot bagasse fiber (ABF) and arrowroot husk fiber (AHF) [14]. However, Rosli *et al.* reported that ABF has a higher cellulose content (45.97%) compared to AHF (37.35%) [19]. Based on this, the present study focused exclusively on extracting nanocellulose from ABF due to its superior cellulose content.

Arrowroot nanocrystalline cellulose was produced through acid hydrolysis following the method outlined

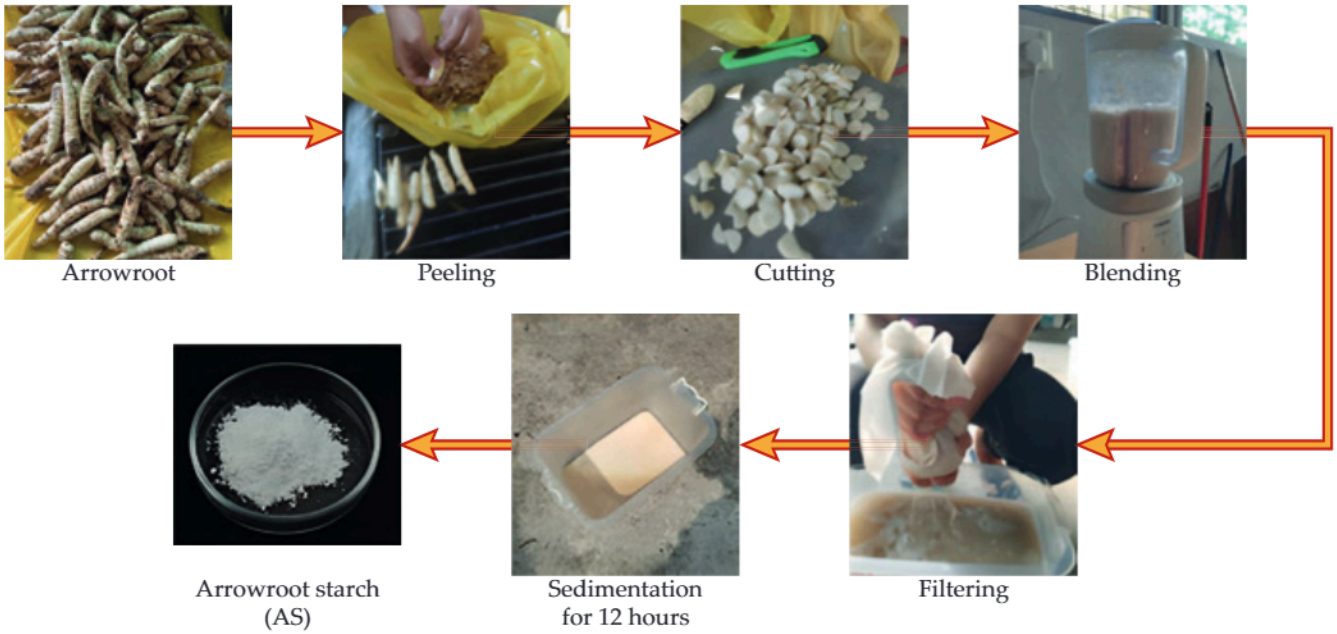

Fig. 3. Process of AS extraction

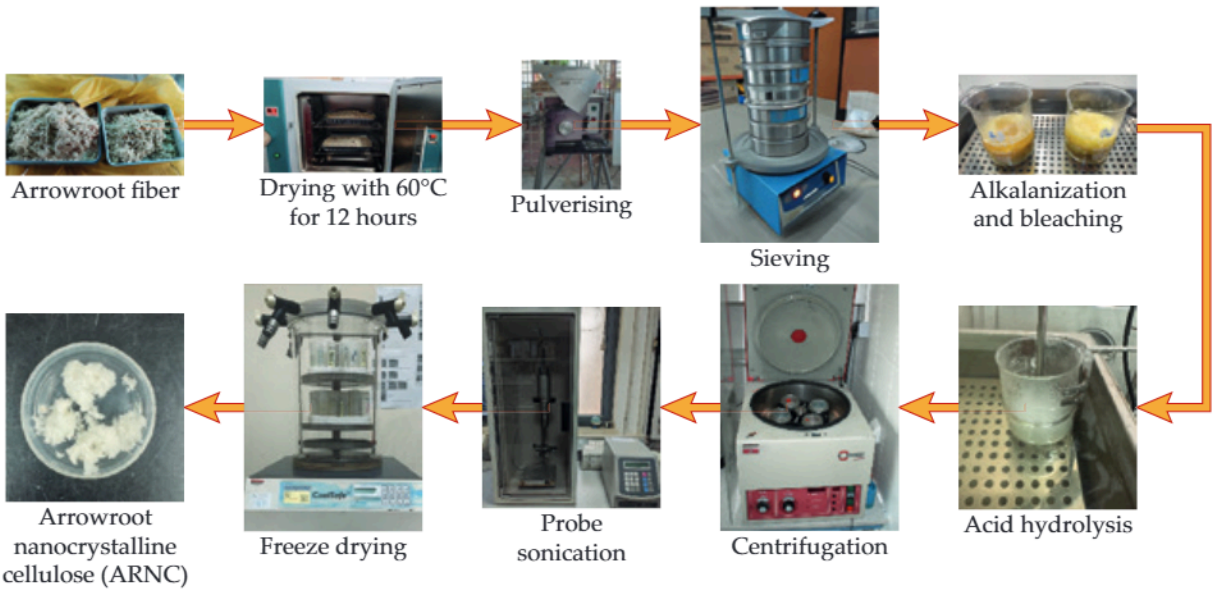

Fig. 4. Process of ARNC extraction

by Ilyas *et al.* [20]. In this process, cellulose was treated with a 60 wt% H_2SO_4 solution at 45°C for 45 min, which was determined to be the optimal reaction time. The ratio of cellulose to acid solution was maintained at 5:100 (wt%) (5 g cellulose to 100 g H_2SO_4). After hydrolysis, the sample was purified by centrifugation at 6,000 rpm for 10 min at 8°, repeated five times to eliminate residual acid. The resulting suspension was then dialyzed with distilled water until a stable pH was achieved. Subsequently, the sample underwent sonication for 30 minutes, followed by freeze-drying, and was stored under cool conditions. The overall extraction process of ARNC is illustrated in Figure 4.

Preparation of biopolymer nanocomposite film

Biopolymer nanocomposite films were fabricated using the conventional solution casting technique. An aqueous suspension of ARNC was first prepared by dispersing ARNC at concentrations ranging from 1 to 3 wt% in distilled water. The film-forming solution of AS was obtained by dissolving 10 g of AS in 180 mL of distilled water. A plasticizer mixture comprising glycerol and sorbitol (30% w/w of starch, in a 1:1 ratio) was then incorporated into the solution under continuous stirring while heating at 80°C for 15 min. After heating, the suspension was allowed to cool, and 50 g of the film-forming solution was poured into petri dishes (13 cm diameter).

The films were dried in an oven at 40°C for 24 h. Pure AS films without ARNC were prepared as AR/ARNC0, while the nanocomposite films containing 1 wt% and 3 wt% ARNC were denoted as ARNC1 and ARNC3, respectively. Following drying, the films were conditioned at 25°C for 24 h, carefully peeled from the dishes, and subsequently stored at 25±3°C and 52% relative humidity for

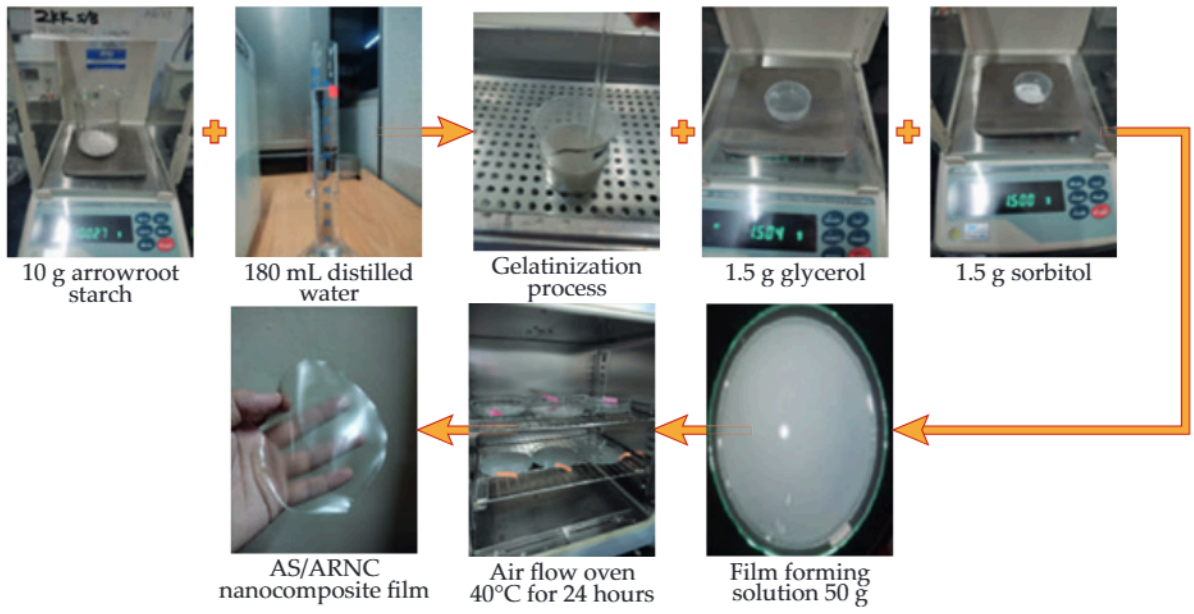

Fig. 5. Biopolymer film preparation process

T a b l e 1. Composition of AS/ARNC films

Sample	AS, g	ARNC, wt%	Sorbitol, wt%	Glycerol, wt%	Distilled water, mL
AS/ARNC0	10	0	15	15	180
AS/ARNC1	10	1	15	15	180
AS/ARNC3	10	3	15	15	180

one week prior to characterization. Figure 5 illustrates the preparation process of AS/ARNC films, and the composite formulations are summarized in Table 1.

Characterization

Mechanical properties

The tensile behaviors of biocomposite samples were evaluated at room temperature using an Instron 3366 tensile machine following the ASTM D882-02 standard. The samples (70 × 10 mm²) were properly fixed between tensile clamps as suggested by Tarique *et al.* [21]. For this test, 3 specimens were test based on the different nanocellulose loading (0, 1, 3 wt%). The gauge length of the samples was initially set to 30 mm, with the testing machine crosshead speed maintained at 2 mm/min. Tensile strength, Young's modulus, and elongation at break were measured for five replicates of each specimen. The mechanical properties were determined based on the average values of these measurements. The collected data were subsequently tabulated and analyzed following the completion of the experiment.

Morphology

The surface structure of the film was analyzed by field emission scanning electron microscopy (FESEM) using a FESEM JEOL JSM-7800F instrument. The fracture surface resulting from the tensile test was used to evaluate the film's microstructure.

Physical properties

A micrometer (Mitutoyo-co, Kawasaki, Japan) with a precision of 0.001 mm was used to measure the thickness of the biopolymer composite film. The thickness of each biopolymer film replicate was determined using the ASTM method F2251 then the mean value was calculated to obtain the actual thickness. The density of the film samples was determined using XS205 Mettler Toledo balance densimeter followed ASTM D792-00. Firstly, the sample was measured to 2 × 2 cm and recorded in air using the XS205 balance. A glass container was then filled with ethanol, and the sample was immersed completely ensuring no air bubbles adhered to its surface. The sample's submerged mass was measured using the balance's built-in density determination function. The balance calculated the density based on the mass difference and the known density of ethanol at the test temperature. The displayed density value was recorded, and adjustments were made for any temperature variations, as necessary. The test was repeated three times for each different load.

Water contents

The moisture content of the film samples was determined following ASTM D664-07. Three replicates of each sample were prepared and weighed to obtain their initial mass (M_i). The samples were then dried in an oven at 105°C for 24 hours and reweighed to obtain the final mass (M_f). The percentage of water content (W_c) was calculated using Equation (1):

$$W_c[\%] = \left(\frac{M_i - M_f}{M_i}\right) \cdot 100 \quad (1)$$

where W_c is the moisture content, M_i is the initial mass of the sample, and M_f is the final mass of the sample.

RESULTS AND DISCUSSION

Physical properties

Thickness of biopolymer nanocomposite film

The thickness measurements of AS/ARNC films demonstrate minor variations in response to various nanocellulose loadings. The AS/ARNC0 sample with 0% nanocellulose, has a thickness of 0.163 mm. The thickness of the film with 1% nanocellulose content (ARNC1) is slightly larger and is 0.169 mm, while the thickness of the film with 3% nanocellulose content (ARNC3) is 0.176 mm. This demonstrated that the film was slightly thickened by the addition of nanocellulose at lower concentrations, as these differences suggest that the biopolymer matrix facilitates better packing and integration. However, the increased thickness at higher concentrations resulted from the accumulation

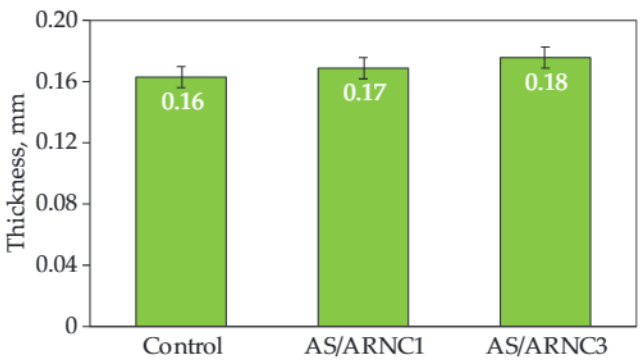

Fig. 6. Thickness with different AS/ARNC biopolymer nanocomposite film

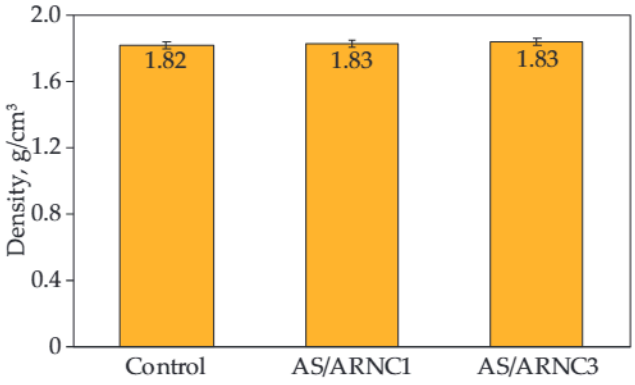

Fig. 7. Density with variety of AS/ARNC biopolymer nanocomposite films

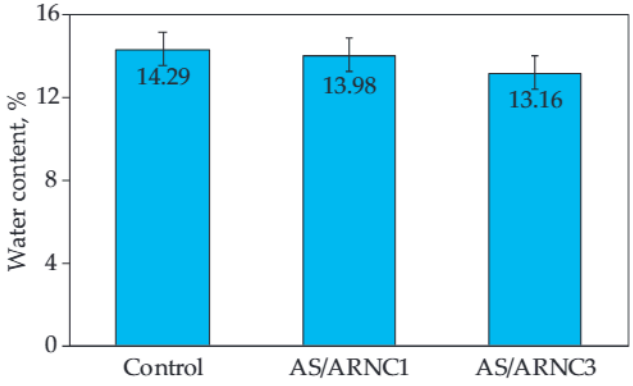

Fig. 8. Water content in AS/ARNC films

and dispersion of nanocellulose fibers within the matrix, resulting in a slightly higher film density [22]. This slight increase in thickness at higher nanocellulose loading does not significantly detract from the film's overall performance but should be considered in applications where precise thickness control is essential [23]. Figure 6 shows thickness of AS/ARNC biopolymer nanocomposite films.

Density

The density of the films increased with the rising concentration of ARNC loadings. Films with higher concentrations of ARNC loading demonstrated higher density compared to those with lower concentrations. The AS/ARNC0 film has the lowest density which is 1.48 g/cm^3 while the highest density is 1.60 g/cm^3 for ARNC3. This is due to the chemical properties of the nanofiller, which features an abundance of hydroxyl groups on the large surface area of ARNCs [24]. These hydroxyl groups facilitate strong interactions during film processing. As these strong interactions among ARNCs were partly disrupted, new, strong interfacial adhesion formed between the ARNC and the AS matrix film [25]. This occurs because nanocellulose fills the interstitial spaces between biopolymer molecules, effectively reducing voids and compacting the material [26]. The densification process is crucial for enhancing the mechanical properties of the film. Generally, as the volume decreased the density of the bio nanofilms increased [27]. Apart from that, this increase in density could potentially lead to improved durability and stability of the films [28]. Figure 7 shows density of AS/ARNC biopolymer nanocomposite films.

Water content

The trend indicates that as ARNC loading increases, the percentage of water content decreases. The water content of the AS/ARNC0 sample, which has no presence of nanocellulose is 14.29%. This value decreases slightly to 13.98% with a 1 wt% nanocellulose loading (ARNC1) and further to 13.16% with a 3 wt% nanocellulose loading (ARNC3). This decrease in water content implies that the film's moisture resistance is improved by ARNC. This impact is a result of several variables. Nanocellulose's high aspect ratio and strong hydrogen bonding capability are expected to result in a denser and more tightly packed film structure, lowering free volume and porosity besides limiting the regions where water molecules might reside [29]. Furthermore, even though nanocellulose is hydrophilic, adding it might make the composite less hydrophilic overall and increase its hydrophobicity [30]. Moreover, a network of nanocellulose could prevent the flow of water molecules through the film by acting as a physical barrier. Figure 8 shows the water content with different AS/ARNC biopolymer nanocomposite films.

Tensile properties

The bar chart presents the influence of nanocellulose loading on the tensile strength of AS-based films. The AS/ARNC0 film, consisting solely of AS without any reinforcement, showed the lowest tensile strength of 2.5 MPa. With the addition of 1 wt% ARNC (AS/ARNC1), the tensile strength increased to 3.4 MPa, demonstrating a marked improvement in mechanical properties. This enhancement is primarily associated with the reinforcing role of nanocellulose, which facilitates more efficient stress transfer within the polymer matrix owing to its high aspect ratio and strong hydrogen bonding interactions with starch chains [31].

Further reinforcement with 3 wt% nanocellulose (AS/ARNC3) results in the highest tensile strength of 4.3 MPa. This shows a progressive strengthening effect with increasing nanocellulose content, suggesting that higher loadings contribute to improved rigidity and network formation within the starch matrix [32]. The error bars indicate reproducibility of the measurements, and the trend confirms that the incorporation of nanocellulose significantly enhances the tensile properties compared to the AS/ARNC0.

The results demonstrate that ARNC acts as an effective reinforcement agent for starch-based films, with tensile strength increasing proportionally to nanocellulose loading. This highlights the potential of such biocomposite

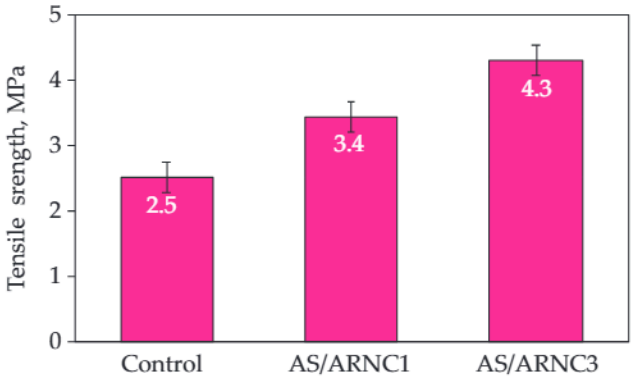

Fig. 9. Tensile strength of AS/ARNC films

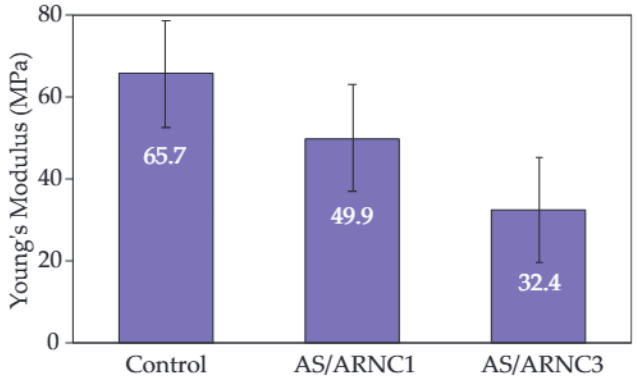

Fig. 10. Young's modulus of AS/ARNC films at different loadings

films for applications requiring improved mechanical stability [33]. Figure 9 shows tensile strength of different AS/ARNC loadings.

Young's modulus

The bar chart illustrates the effect of ARNC loading on the stiffness of arrowroot starch-based films, as expressed by Young's modulus. The AS/ARNC0 sample, without ARNC reinforcement, exhibited the highest modulus value at 65.7 MPa, indicating that the neat starch film is rigid and brittle. This high stiffness corresponds with its low elongation at break, as starch films tend to resist deformation but fail quickly under stress [34].

When 1 wt% ARNC was incorporated into the matrix (AS/ARNC1), the Young's modulus decreased to 49.9 MPa. This reduction suggests that the addition of nanocrystalline cellulose reduced the stiffness of the film, making it less brittle and more flexible. The ARNC likely disrupted the dense starch molecular packing by introducing new interactions between the starch and cellulose nanocrystals, allowing greater polymer chain mobility [35].

At a higher loading of 3 wt% ARNC (AS/ARNC3), the modulus further decreased to 32.5 MPa, representing a substantial drop in stiffness compared to the AS/ARNC0. The results reveal an inverse relationship between elongation at break and Young's modulus [36]. While ARNC reinforcement significantly enhanced flexibility and ductility, it simultaneously reduced stiffness [37]. This indicates a trade-off in mechanical properties, where higher ARNC loading favors flexibility and toughness at the expense of rigidity [38]. Figure 10 shows Young's modulus of AS/ARNC films.

Elongation at break

Fig. 11 shows the effect of ARNC loading on the elongation at break of arrowroot starch-based films. The AS/ARNC0 sample, without any ARNC reinforcement, exhibited the lowest elongation at break (13.4%), indicating poor flexibility and ductility of the neat starch film. This brittleness is typical of starch-based films due to their rigid polymer chains and weak molecular interactions [39]. Upon the addition of 1 wt% ARNC (AS/ARNC1), the elongation at break increased significantly to 38.9%. This improvement demonstrates that ARNC acted as an efficient reinforcing agent, promoting better stress transfer and enhancing the flexibility of the starch matrix [40]. The nanocrystalline cellulose likely disrupted the strong intermolecular hydrogen bonding among starch molecules, thereby allowing greater molecular mobility and ductility [41]. Further increasing the ARNC loading to 3 wt% (AS/ARNC3) resulted in the highest elongation at break value of 45%. This indicates that a higher concentration of well-dispersed ARNC improved the structural integrity of the film by forming a reinforcing network that allowed better distribution of applied stress. However, the improvement also suggests that at this concentration, agglomeration did not critically hinder flexibility, which is consistent with the FESEM observations where some agglomeration was present but not dominant [42].

Table 2 shows that the tensile strength of ARNC-reinforced AS is 2.47–4.31 MPa, which is higher than that of glycerol-reinforced AS, but significantly lower than the tensile strength of arrowroot, poly(vinyl alcohol) (PVA) and polyhydroxyalkanoate (PHA) composites, which typically exceed 11 MPa. The elongation at break of

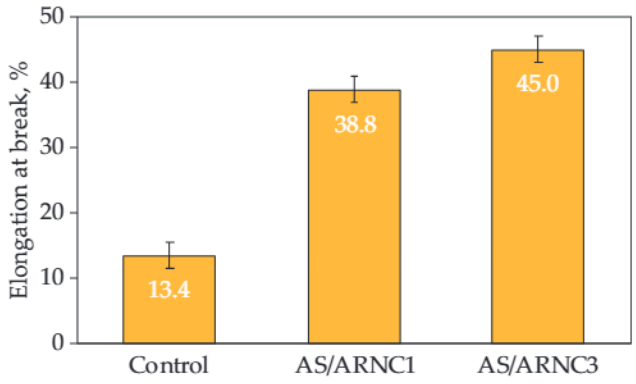

Fig. 11. Elongation at break of AS/ARNC films

T a b l e 2. Comparison of mechanical properties of various composites

Composite	Tensile strength MPa	Elongation at break %	Young's modulus MPa	Ref.
Arrowroot fiber reinforced AS	2.4–15.2	6.2–46.6	52–1072	[21]
Polyvinyl alcohol (PVA) reinforced AS	11.8–18.5	17.5–184.3	–	[43]
AS reinforced glycerol	2.15–2.68	41.0–62.9	–	[43]
Polyhydroxyalkanoate (PHA) reinforced AS	11.8–18.5	17.5–184.3	–	[44]

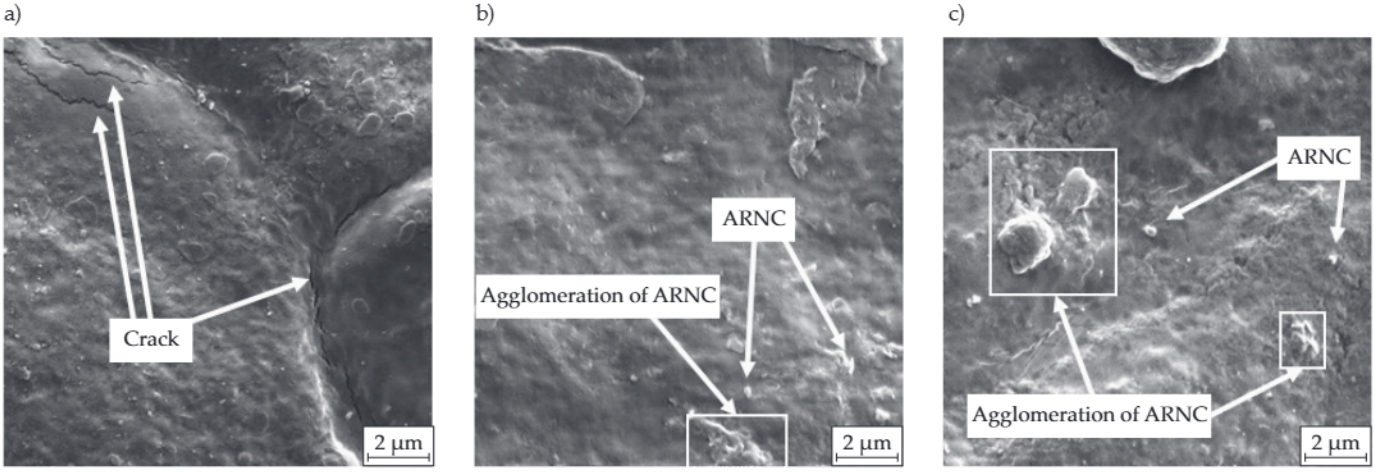

Fig. 12. FESEM images of AS/ARNC films: a) AS/ARNC0, b) AS/ARNC1, c) AS/ARNC3, magnification ×10,000

ARNC-reinforced AS ranges from 13.4 to 45 MPa, which is in the same range as for arrowroot/AS systems and partially in the lower half of the PVA and PHA range, resulting in moderate elasticity but not as ductile as glycerol-reinforced AS. The Young's modulus, from 32.5 to 65.7 MPa, is significantly lower than that of arrowroot reinforced AS, demonstrating that the tested material is less stiff and more flexible, which is also typical for flexible films made of nanocellulose.

Microstructure analysis

Figure 12 shows FESEM micrographs results with 10,000 magnifications of AS/ARNC nanocomposite films. In Figure 12a, distinct cracks are visible on the surface of the film. The presence of these cracks indicates brittle fracture behavior within the material, which is commonly associated with poor interfacial bonding between the ARNC and the starch matrix. When stress is applied, insufficient adhesion prevents effective stress transfer from the matrix to the nanocrystals, causing localized stress accumulation that eventually initiates cracks [45]. These cracks can propagate further, compromising the mechanical integrity of the film and leading to a reduction in tensile strength and durability [46].

In Figure 12b, both individual ARNC particles and agglomerated regions are observed. The well-dispersed ARNC particles provide reinforcement to the matrix, enhancing stiffness, tensile strength, and barrier performance of the composite [47]. This beneficial effect is due to the high aspect ratio and crystallinity of the nanocrystals, which allow them to act as efficient stress carriers [48]. However, the agglomerated clusters of ARNC highlight an issue of poor dispersion, often resulting from strong hydrogen bonding interactions between the nanocrystals [49]. These clusters act as stress concentrators, creating weak points in the structure that can initiate microcracks and reduce the uniform stress distribution within the film [50].

In Figure 12c, larger agglomerates of ARNC are more apparent, along with individual nanocrystals distributed across the surface. The presence of such agglomeration further suggests incomplete dispersion during film preparation, which can negatively affect the homogeneity of the composite [51]. While some reinforcement effect is still expected from the well-dispersed ARNC, the larger clusters reduce the overall efficiency of reinforcement by creating defects that may lead to mechanical failure under load [52]. These observations imply that further optimization of the dispersion process, possibly through surface modification of ARNC or improved mixing techniques, is required to achieve a more uniform structure and improved mechanical performance of the film [53].

CONCLUSIONS

The addition of ARNC was shown to improve the physical and mechanical properties of arrowroot starch-based biopolymer films. An increase in film density was observed, while water absorption decreased, thereby increasing moisture resistance. The films showed a significant increase in tensile strength (from 2.5 to 4.3 MPa).

At the same time, the films exhibited greater flexibility and ductility, as the elongation at break increased from 13.4% to 45%, and Young's modulus decreased from 65.7 MPa to 32.5 MPa. FESEM analysis indicated that ARNC is an effective reinforcing agent, but its agglomeration at higher concentrations can pose a challenge to achieving a uniform film structure. Taken together, these results indicate the potential success of ARNC as a natural reinforcing material to produce sustainable biopolymer films with high strength, durability, and barrier properties in various applications.

ACKNOWLEDGEMENTS

The authors thank The Ministry of Higher Education Malaysia (MoHE) for financing this work under the Fundamental Research Grant Scheme (FRGS), with project code of FRGS/1/2023/TK09/UPM/01/3/5540599.

Authors contribution

A.H.M.F. – writing-original draft, writing-review and editing, data curation, resources, methodology, conceptualization; S.M.S. – supervision, funding acquisition, conceptualization; E.S.Z. – supervision; A.A. – supervision; M.F.M.I.H. – writing-review and editing, data curation, resources, methodology, conceptualization; V.U.S. – supervision.

Funding

The authors wish to thank The Ministry of Higher Education Malaysia (MoHE) for financing this work under the Fundamental Research Grant Scheme (FRGS), with project code of FRGS/1/2023/TK09/UPM/01/3/5540599.

Conflict of interest

The authors declare no conflict of interest.

REFERENCES

[1] Manu T., Nazmi A.R., Shahri B. *et al.*: *Materials Today: Communications* **2022**, *31*, 103308. https://doi.org/10.1016/j.mtcomm.2022.103308

[2] Bangar S.P., Whiteside W.S.: *International Journal of Biological Macromolecules* **2021**, *185*, 849. https://doi.org/10.1016/j.ijbiomac.2021.07.017

[3] Udayakumar G.P., Muthusamy S., Selvaganesh B. *et al.*: *Journal of Environmental Chemical Engineering* **2021**, *9(4)*, 105322. https://doi.org/10.1016/j.jece.2021.105322

[4] Kaur P., Sharma N., Munagala M. *et al.*: *Frontiers in Nanotechnology* **2021**, *3*, 747329. https://doi.org/10.3389/fnano.2021.747329

[5] Xu Y., Wu Z., Li A. *et al.*: *Polymers* **2024**, *16(3)*, 423. https://doi.org/10.3390/polym16030423

[6] Tarique J., Sapuan S.M., Khalina A.: *Scientific Reports* **2021**, *11*, 13900. https://doi.org/10.1038/s41598-021-93094-y

[7] Khan A., Sapuan S.M., Husna N.: "A review on arrowroot fiber reinforced polymer composites" in "Plant Tuber and Root-Based Biocomposites", Woodhead Publishing, Cambridge, 2025, p. 227. https://doi.org/10.1016/B978-0-443-14126-3.00011-4

[8] Fadhallah E.G., Indraningtyas L., Mardhiyah R. *et al.*: *MOJ Ecology & Environmental Sciences* **2024**, *9(1)*, 1. https://doi.org/10.15406/mojes.2024.09.00299

[9] de Oliveira Filho J.G., Albiero B.R., Cipriano L. *et al.*: *Cellulose* **2011**, *28*, 6499. https://doi.org/10.1007/s10570-021-03945-0

[10] Tarique J., Sapuan S.M., Khalina A. *et al.*: *International Journal of Biological Macromolecules* **2022**, *213*, 1. https://doi.org/10.1016/j.ijbiomac.2022.05.104

[11] Abdillah A.A., Charles A.L.: International Journal of Biological Macromolecules 2021, 191, 618. https://doi.org/10.1016/j.ijbiomac.2021.09.141

[12] Ilyas R.A., Sapuan S.M., Norrrahim M.N.F.: "Nanocellulose-Reinforced Thermoplastic Starch Composites: Sustainable Materials for Packaging:, Walter de Gruyter GmbH & Co KG, 2023.

[13] Amante P.R., Santos E.C.Z., da Veiga Correia V.T. *et al.*: *Journal of Culinary Science & Technology* **2021**, *19(6)*, 513. https://doi.org/10.1080/15428052.2020.1791295

[14] Tarique J., Sapuan S.M., Zainudin E.S. *et al.*: *Materials Today: Proceedings* **2023**, *74(3)*, 411. https://doi.org/10.1016/j.matpr.2022.11.136

[15] Hazrol M.D., Sapuan S.M., Ilyas R.A. *et al.*: *Heliyon* **2023**, *9(4)*, e15153. https://doi.org/10.1016/j.heliyon.2023.e15153

[16] Sartika M., Rampe F.R., Parinduri S.Z.D.M. *et al.*: *IOP Conference Series: Earth and Environmental Science* **2022**, *1115*, 012075. https://doi.org/10.1088/1755-1315/1115/1/012075

[17] Malki M.K.S., Wijesinghe J.A.A.C., Ratnayake R.H.M.K. *et al.*: *Heliyon* **2023**, *9(9)*, e20033. https://doi.org/10.1016/j.heliyon.2023.e20033

[18] Subando T.R., Pranoto Y., Witasari L.D.: *Research Square* **2023**, *(preprint)*. https://doi.org/10.21203/rs.3.rs-2440776/v1

[19] Rosli N., Sapuan S., Leman Z. *et al.*: *Journal of Natural Fibre Polymer Composites* **2022**, *1*, 4.

[20] Ilyas R.A., Sapuan S.M., Ishak M.R. et al.: "Characterization of Sugar Palm Nanocellulose and Its Potential for Reinforcement with a Starch-Based Composite" in " Sugar Palm Biofibers, Biopolymers, and Biocomposites", CRC Press, Boca Raton 2018, p. 189.

https://doi.org/10.1201/9780429443923-10
[21] Tarique J., Zainudin E.S., Sapuan S.M. *et al.*: *Polymers* **2022**, *14(3)*, 388. https://doi.org/10.3390/polym14030388
[22] Yang Y., Luo C.L., Chen X.D. *et al.*: *Composites Science and Technology* **2023**, *233*, 109913. https://doi.org/10.1016/j.compscitech.2023.109913
[23] Guivier M., Almeida G., Domenek S. *et al.*: *Carbohydrate Polymers* **2023**, *312*, 120761. https://doi.org/10.1016/j.carbpol.2023.120761
[24] Benselfelt T., Kummer N., Nordenström M. *et al.*: *ChemSusChem* **2023**, *16(8)*, e202201955. https://doi.org/10.1002/cssc.202201955
[25] Tay C.H., Mazlan N., Wayayok A. *et al.*: *Materials Today: Proceedings* **2022**, *66(5)*, 2873. https://doi.org/10.1016/j.matpr.2022.06.550
[26] Syafiq R., Sapuan S.M., Zuhri M.R.M.: *Journal of Materials Resarch and Technology* **2021**, *11*, 144. https://doi.org/10.1016/j.jmrt.2020.12.091
[27] Talebi H., Ghasemi F.A., Ashori A.: J*ournal of Elastomers & Plastics* **2021**, *54(1)*, 22. https://doi.org/10.1177/00952443211017169
[28] Babaee M., Garavand F., Rehman A. *et al.*: *International Journal of Biological Macromolecules* **2022**, *195*, 49. https://doi.org/10.1016/j.ijbiomac.2021.11.162
[29] Jing S., Wu L., Siciliano A.P. *et al.*: *ACS Nano* **2023**, *17(22)*, 22196. https://doi.org/10.1021/acsnano.3c06773
[30] Solhi L., Guccini V., Heise K. *et al.*: *Chemical Reviews* **2023**, *123(5)*, 1925. https://doi.org/10.1021/acs.chemrev.2c00611
[31] Othman S.H., Nordin N., Azman N.A.A. *et al.*: *International Journal of Biological Macromolecules* **2021**, *183*, 1352. https://doi.org/10.1016/j.ijbiomac.2021.05.082
[32] Zhang J., Zou F., Tao H. *et al.*: *Industrial Crops and Products* **2023**, *194*, 116358. https://doi.org/10.1016/j.indcrop.2023.116358
[33] Srivastava K.R., Dixit S., Pal D.B. *et al.*: *Environmental Technology & Innovation* **2021**, *21*, 101312. https://doi.org/10.1016/j.eti.2020.101312
[34] Wassgren J., Clarke B.R., Messikh M.B. *et al.*: *Carbohydrate Polymers* **2025**, *348(B)*, 122839. https://doi.org/10.1016/j.carbpol.2024.122839
[35] Ghasemi S., Ghasemi B., Espahbodi A. *et al.*: *Journal of Composite Materials* **2023**, *57(8)*, 1449. https://doi.org/10.1177/00219983231155595
[36] Ghasemi S., Espahbodi A., Gharib N. *et al.*: *Industrial Crops and Products* **2023**, *206*, 117703. https://doi.org/10.1016/j.indcrop.2023.117703
[37] Wang Y., Yu Z., Dufresne A. *et al.*: *ACS Nano* **2021**, *15(12)*, 20148. https://doi.org/10.1021/acsnano.1c08100
[38] S. Çavdar, Sepetcioglu H., Karagöz I.: *Cellulose* **2024**, *31*, 9715. https://doi.org/10.1007/s10570-024-06193-0
[39] Do T.V.V., Tran N.B.A., Nguyen-Thai N.U.: *Polymer Composites* **2023**, *44(4)*, 2287. https://doi.org/10.1002/pc.27243
[40] Feng K., Dong C., Gao Y. *et al.*: *ACS Sustainable Chemistry and Engineering* **2021**, *9(19)*, 6764. https://doi.org/10.1021/acssuschemeng.1c00948
[41] Perdoch W., Cao Z., Florczak P. *et al.*: *Molecules* **2022**, *27(15)*, 4696. https://doi.org/10.3390/molecules27154696
[42] Hu C., Zhou Y., Zhang T. *et al.*: *Fibers and Polymers* **2021**, *22*, 2187. https://doi.org/10.1007/s12221-021-0903-3
[43] de Almeida Nascimento J.A., dos Santos A.F., Lima Silva I.D. *et al.*: *Journal of Macromolecular Science, Part B* **2021**, *60(12)*, 1045. https://doi.org/10.1080/00222348.2021.1949836
[44] Wu C.S., Liao H.T.: *Materials Science and Engineering: C* **2017**, *70(1)*, 54. https://doi.org/10.1016/j.msec.2016.08.067
[45] Trivedi A.K., Kumar A., Gupta M.K.: *Materials Today: Proceedings* **2023**, *78(1)*, 48. https://doi.org/10.1016/j.matpr.2022.11.038
[46] Sihag S., Pal J., Yadav M.: *Journal of Water and Environmental Nanotechnology* **2022**, *7(3)*, 317. https://doi.org/10.22090/jwent.2022.03.007
[47] Ismail F., Othman N.E.A., Wahab N.A.: *Journal of Advanced Research in Fluid Mechanics and Thermal Sciences* **2023**, *102(2)*, 120. https://doi.org/10.37934/arfmts.102.2.120128
[48] Bakr E.A., Gaber M., Saad D.R. *et al.*: *International Journal of Biological Macromolecules* **2023**, *230*, 123315. https://doi.org/10.1016/j.ijbiomac.2023.123315
[49] Singh H., Kumar Verma A., Kumar Trivedi A. *et al.*: *Materials Today: Proceedings* **2024**, *106*, 1. https://doi.org/10.1016/j.matpr.2023.02.300
[50] Sainorudin M.H., Abdullah N.A., Asmal Rani M.S. *et al.*: *Current Nanoscience* **2022**, *18(1)*, 68. http://doi.org/10.2174/1573413717666210216115609
[51] Sheetal, Sihag S., Yadav M. *et al.*: *Journal of Water and Environmental Nanotechnology* **2022**, *7(1)*, 1. https://doi.org/10.22090/jwent.2022.01.001
[52] Ilyas R.A., Sapuan S., Atikah M. *et al.*: *Textile Research Journal* **2020**, *91(1-2)*, 152. https://doi.org/10.1177/0040517520932393
[53] Shalauddin M., Akhter S., Basirun W.J. *et al.*: *Surfaces and Interfaces* **2022**, *34*, 102385. https://doi.org/10.1016/j.surfin.2022.102385

Received 3 IX 2025.
Accepted 14 XI 2025.